Spectral-domain optical coherence reflectometric sensor for highly sensitive molecular detection

Chulmin Joo[1,2,*] and Johannes F. de Boer[2,3]

[1]*Department of Mechanical Engineering, Massachusetts Institute of Technology, Cambridge, Massachusetts 02139, USA*

[2]*Wellman Center for Photomedicine, Massachusetts General Hospital, Boston, Massachusetts 02114, USA*

[3]*deboerehelix.mgh.harvard.edu*

[*]*Corresponding author: cmjoo@mit.edu*

Received April 18, 2007; revised July 3, 2007; accepted July 11, 2007; posted July 16, 2007 (Doc. ID 82235); published August 7, 2007

We describe what we believe to be a novel use of spectral-domain optical coherence reflectometry (SD-OCR) for highly sensitive molecular detection in real time. The SD-OCR sensor allows identification of a sensor surface of interest in an OCR depth scan and monitoring the phase alteration due to molecular interaction at that surface with subnanometer optical thickness sensitivity. We present subfemtomole detection sensitivity for etching of SiO_2 molecules and demonstrate its application as a biosensor by measuring biotin-streptavidin binding in a microfluidic device. © 2007 Optical Society of America

OCIS codes: 110.4500, 120.3180, 280.0280.

Real-time detection of minute traces of molecules on activated sensor surfaces is of great importance in many applications such as medical diagnostics, disease screening, and environmental monitoring. Such detection has often been conducted by fluorescence methods [1]. These label-based techniques could potentially achieve single molecular level detection but require additional specimen preparation, which is time consuming and may affect molecular structures or interaction properties. Label-free methods detect physical absorption of molecules on a sensor surface. Surface plasmon resonance (SPR) [2] and resonant microcavity [3] sensors exploit the change of the resonant SPR angle and the optical frequency due to the alteration of refractive index at the sensor surface upon the molecular absorption, respectively.

Optical interferometric methods for molecular recognition have been extensively explored since they enable label-free detection with high speed and sensitivity. Those techniques include porous silicon-based interferometry [4], integrated Young's interferometry [5], and the optical biological compact disc (BioCD) [6,7]. The spectral-domain optical coherence reflectometer (SD-OCR) is an optical ranging technique employing low-coherence spectral interferometry to measure the position of reflective surfaces in a specimen relative to a reference mirror. Recent studies revealed that SD-OCR has improved speed and phase stability compared with time-domain OCR methods mainly due to the absence of mechanical scanning of the reference mirror [8–10]. SD-OCR has been successfully utilized to investigate cellular dynamics [11] and neural activity [12], and its extension to imaging modality, spectral-domain optical coherence tomography was used to image biological cells [13] and tissues [14], exploiting its improved phase stability.

We present a novel application of spectral-domain optical coherence reflectometry to real-time detection of molecular interaction. Based on the low-coherence interferometer, the SD-OCR sensor allows the identification of the sensor surface of interest by means of coherence gating and confines the reflection signal from the sensor surface to within the coherence length of the source. The signal related to the surface is thus not influenced by the reflection from the other surfaces but detects the optical thickness change due to molecular absorption or desorption at that surface. The sensing region for the SD-OCR sensor can be as small as the diffraction-limited beam spot size, enabling detection with significantly reduced sample volumes. In this Letter, we demonstrate the sensitivity of SD-OCR sensor by measuring the optical thickness change of SiO_2 layer as it is etched by diluted hydrofluoric acid solution and present its utility as a biosensor by monitoring biotin–streptavidin binding in a microfluidic channel.

Figure 1 depicts a schematic of an SD-OCR sensor. A broadband 800 nm Kerr-lens mode-locked laser with a bandwidth of ~130 nm in full width at half-maximum (FWHM) (FemtoLasers, Austria) is employed as a light source, which gives 2–3 μm in coherence length in air. The beam at the sample arm is focused onto molecule-coupled sensor surface via a microscope objective (Carl Zeiss, 5×, NA=0.13) with a measured lateral resolution of ~2.5 μm in FWHM. The backreflected beams from the interfaces are recoupled to the interferometer to produce an interference spectrum, which is then detected by a custom-built spectrometer at a maximum frequency of 29 kHz [14]. A complex-valued depth information $F(z)$ is obtained by a discrete Fourier transform of the interference spectrum, and the intensity and phase at depth z can be extracted as $I(z)=|F(z)|^2$ and $\phi(z)=\tan^{-1}[\mathrm{Im}(F(z))/\mathrm{Re}(F(z))]=2(2\pi/\lambda_0)\Delta p(z)$, respectively. Here, λ_0 is the center wavelength of the source, and $\Delta p(z)$ is the optical path delay between reference and sensor surface at depth z. The depth-resolved intensity information is used to locate a spe-

0146-9592/07/162426-3/$15.00

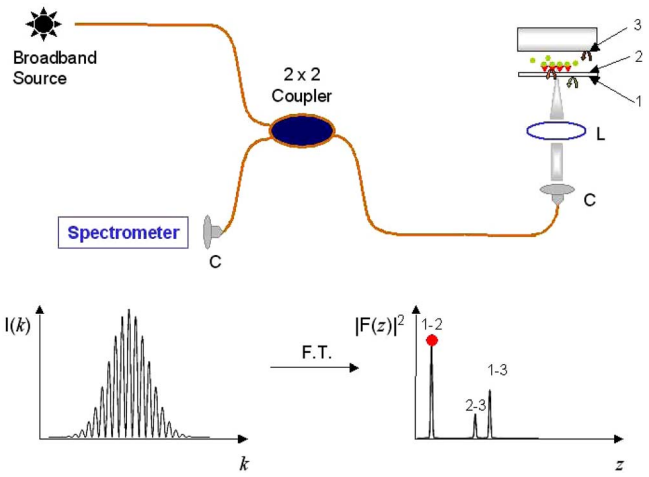

Fig. 1. (Color online) Schematic of the SD-OCR sensor. The spectrometer measures the interference spectrum of the reflected beams from the interfaces, which is then Fourier transformed to obtain depth-resolved intensity and phase information. Using the intensity information, the interference signal related to the molecule-coupled sensor surface is located (circle labeled 1-2), and the phase of that signal is examined to monitor molecular absorption. The other interference signals denoted by 2-3 and 1-3 are not used since their phase information is also influenced by the reflection from other surfaces and the change in solution refractive index. C, collimator; L, focusing lens.

cific interference signal related to the molecule-coupled sensor surface, and the phase (or optical thickness) of that signal is monitored to examine molecular absorption at that surface. The other interference signals denoted by "2-3" and "1-3" in Fig. 1 are not selected because their phase information is also affected by the reflection from the other surfaces and the change in the refractive index of solution. In the shot-noise-limited regime, the phase sensitivity for SD-OCR can be expressed as an explicit function of signal-to-noise ratio (SNR) as $\langle \Delta\phi^2 \rangle \approx 1/(2\mathrm{SNR})$ [11,15], and we recently reported ~25 pm at a measured SNR of 100.4 dB [13].

The capability of the SD-OCR sensor for detecting traces of small molecules was first assessed by examining the etching process of an SiO_2 layer by a diluted hydrofluoric (HF) acid solution. SiO_2 can be regarded as a representative of small molecules with its molecular weight (MW) of ~60 Da, which is much less than that of bovine serum albumin [(BSA), MW: 60 kDa]. For measurement, a SiO_2-bottom container was filled with de-ionized water, and then a diluted HF solution was introduced into the container to obtain a desired HF concentration. Figure 2(a) shows the change of optical thickness at an HF volume concentration of ~0.07%. The sampling rate was 50 Hz. It can be noted that the optical thickness decreases significantly upon injection of the HF solution, giving a measured etch rate of ~51 nm/min. We also examined the etch rate as a function of HF volume concentration [Fig. 2(b)]. It shows a dramatic etch rate increase when HF concentration is more than 0.02%, which has not been observed in the literature to our knowledge. The noise equivalent optical thickness change (δp) in this experiment was ~0.1 nm at a

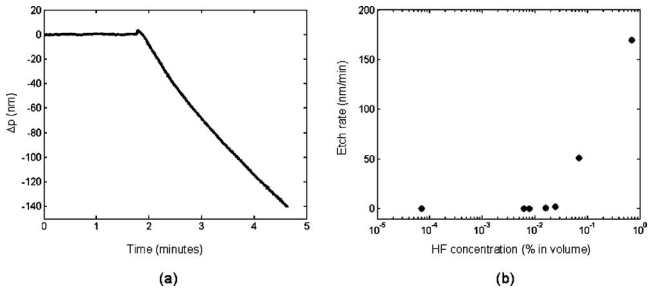

Fig. 2. Real-time detection of SiO_2 etch by diluted HF solutions. (a) Optical thickness change was measured as a function of time at an HF volume concentration of 0.07%. The etch rate was measured as ~51 nm/min. (b) Etch rate as a function of HF volume concentration was examined, showing a dramatic increase at more than 0.02% in HF concentration.

SNR of 57 dB, whereas the theoretical sensitivity is ~64 pm in air at this SNR. The difference may be due to external disturbances such as vibration during the measurement. Using the weight density of 2.2 g/cm^3 [16] and the refractive index of 1.46 for SiO_2, we estimate the surface density and the optical thickness of one monolayer as $\sim 8 \times 10^{14}$ cm^{-2} and 0.51 nm, respectively, assuming that a single SiO_2 molecule occupies a cubic volume. The noise-equivalent thickness can then be approximated as ~0.2 layer, which corresponds to ~0.05 fmol on the sensor surface.

The SD-OCR sensor was further applied to real-time molecular detection in a microfluidic channel. A single-channel microfluidic device was constructed from a coverslip and plasma desorption mass spectrometry polydimethylsiloxane (PDMS) using standard PDMS casting and bonding techniques [17], and the channel was 100 μm wide, 30 μm deep, and 50 mm long. The inner channel of the device was functionalized by a low concentration biotinylated BSA solution [(bBSA), 250 nM). The phase change was recorded at a sampling rate of 50 Hz and then processed by a moving-average filter with a size of 10 points (time constant: 200 ms). Figure 3(a) shows the experimental result for the bBSA-activated fluidic

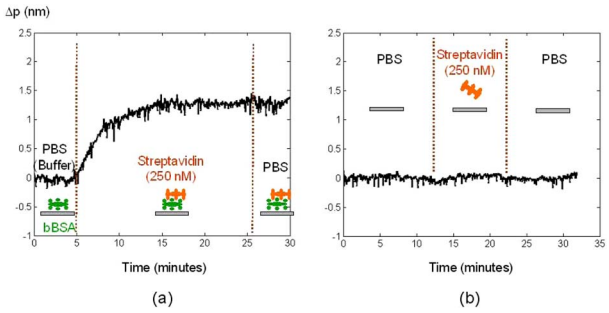

Fig. 3. (Color online) Measured bBSA-streptavidin binding in a microfluidic device by the SD-OCR sensor. Using bBSA-activated surface, the introduction of streptavidin (250 nM) led to an optical thickness increase due to the binding of streptavidin to the bBSA layer in the channel. However, in the case of a nonfunctionalized fluidic channel, even with the same concentration of streptavidin solution, we did not observe a noticeable signal change.

channel. Initially, the introduction of buffer solution [phosphate-buffered saline, (PBS)] did not change the optical thickness, but a noticeable change was observed after the streptavidin solution with a concentration of 250 nM flowed through the device. This optical thickness change is due to the binding of streptavidin to the immobilized bBSA layer, and its magnitude was measured as ~1.3 nm at the equilibrium state. The discrepancy between the measured optical thickness and the size of streptavidin (4–5 nm) as reported in [18] may be in part accounted by the incomplete surface coverage of bBSA layer over the sensing region. After ~20 min, we switched back to PBS and could observe no signal change, which proves strong binding between bBSA and streptavidin. We also conducted a control experiment with a nonactivated channel [Fig. 3(b)]. In this case, the introduction of the streptavidin solution with the same concentration did not induce an optical thickness change, demonstrating specific binding affinity of streptavidin to biotin.

The extension of SD-OCR sensor to multiplexed protein/DNA assays can be achieved by incorporating a scanning device and a sensor surface with different protein/DNA patterns. Since its lateral resolution is diffraction limited, an SD-OCR sensor can detect hundreds to thousands of activated sites to monitor spatially distributed reactions with high spatial and temporal resolution. Moreover, due to its 3D imaging capability, we may envision 3D bioassay with a stack of sensor surfaces, enabling massive 3D protein screening. Including a new active binding site on a sensor surface can easily allow the detection of new chemical and biological species.

In summary, a spectral-domain optical coherence reflectometric sensor was presented as a novel optical method for real-time molecular recognition. The SD-OCR sensor utilizes the coherence gating of low-coherence interferometer to identify the sensor surface of interest and measures its phase alteration for molecular absorption or desorption without the effect of other surfaces and the solution concentration fluctuation. As a proof of concept, the SD-OCR sensor demonstrated subfemtomole detection sensitivity for SiO_2, and was further applied to detect bBSA-streptavidin binding in a microfluidic channel. With further studies on molecular patterning on a sensor surface and with the inclusion of the imaging capability, the SD-OCR sensor may serve as a powerful tool to bioassay.

This research was supported in part by research grants from Center for Integration of Medicine and Innovative Technology, National Institutes of Health (R01 RR19768, EY14975), and the U.S. Department of Defense (F4 9620-01-1-0014).

References

1. D. W. Pierce, N. Hom-Booher, and R. D. Vale, Nature **388**, 338 (1997).
2. J. Homola, S. S. Yee, and G. Gauglitz, Sens. Actuators B **54**, 3 (1999).
3. F. Vollmer, D. Braun, A. Libchaber, M. Khoshsima, I. Teraoka, and S. Arnold, Appl. Phys. Lett. **80**, 4057 (2002).
4. V. S.-Y. Lin, K. Motesharei, K.-P. S. Dancil, M. J. Sailor, and M. R. Ghadiri, Science **278**, 840 (1997).
5. A. Brandenburg, R. Krauter, C. Knzel, M. Stefan, and H. Schulte, Appl. Opt. **39**, 6396 (2000).
6. L. Peng, M. M. Varma, F. E. Regnier, and D. D. Nolte, Appl. Phys. Lett. **86**, 183902 (2005).
7. M. Zhao, D. Nolte, W. Cho, F. Regnier, M. Varma, G. Lawrence, and J. Pasqua, Clin. Chem. **52**, 2135 (2006).
8. R. Leitgeb, C. K. Hitzenberger, and A. F. Fercher, Opt. Express **11**, 889 (2003).
9. J. F. de Boer, B. Cense, B. H. Park, M. C. Pierce, G. J. Tearney, and B. Bouma, Opt. Lett. **28**, 2067 (2003).
10. M. Choma, M. Sarunic, C. Yang, and J. A. Izatt, Opt. Express **11**, 2183 (2003).
11. M. A. Choma, A. K. Ellerbee, C. Yang, T. L. Creazzo, and J. A. Izatt, Opt. Lett. **30**, 1162 (2005).
12. T. Akkin, C. Joo, and J. F. de Boer, Biophys. J. **93**, 1347 (2007).
13. C. Joo, T. Akkin, B. Cense, B. H. Park, and J. F. de Boer, Opt. Lett. **30**, 2131 (2005).
14. N. Nassif, B. Cense, B. H. Park, M. Pierce, S. Yun, B. Bouma, G. Tearney, T. Chen, and J. F. de Boer, Opt. Express **12**, 367 (2004).
15. B. H. Park, M. C. Pierce, B. Cense, S.-H. Yun, M. Mujat, G. Tearney, B. Bouma, and J. F. de Boer, Opt. Express **13**, 3931 (2005).
16. D. R. Lide, ed., *Handbook of Chemistry and Physics* (CRC, 2005).
17. G. M. Whitesides, Nature **442**, 368 (2006).
18. A. Arakaki, S. Hideshima, T. Nakagawa, D. Niwa, T. Tanaka, T. Matsunaga, and T. Osaka, Biotechnol. Bioeng. **88**, 543 (2004).